Shear rheology of fluid interfaces: Closing the gap between macro- and micro-rheology

Eduardo Guzmán,[1,2,*] Javier Tajuelo,[3,§] Juan Manuel Pastor,[4] Miguel Ángel Rubio,[3] Francisco Ortega,[1,2] Ramón G. Rubio,[1,2,*]

[1] *Departamento de Química Física I, Universidad Complutense de Madrid, Ciudad Universitaria s/n. 28040 Madrid, Spain*

[2] *Instituto Pluridisciplinar, Universidad Complutense de Madrid, Paseo Juan XXIII 1, 28040 Madrid, Spain*

[3] *Departamento de Física Fundamental, Universidad Nacional de Educación a Distancia, Paseo Senda del Rey 9, 28040 Madrid, Spain*

[4] Grupo de Sistemas Complejos, Escuela Técnica Superior de Ingeniería Agronómica, Alimentaria y Biosistemas, Universidad Politécnica de Madrid, 28040-Madrid (Spain)

[§] *Current address: Departamento de Física Aplicada, Universidad de Granada, 18071 Granada, Spain*

Published in Current Opinion in Colloid and Interface Science 37 (2018) 33-48

https://doi.org/10.1016/j.cocis.2018.05.004

* To whom correspondence should be addressed: eduardogs@quim.ucm.es (EG) and rgrubio@quim.ucm.es (RGR)

Abstract

For many years the determination of the shear viscosity of interfacial layers has been source of strong controversy. This is mainly because different techniques provided different values of such parameter, which leads in many cases to a puzzling interpretation of the experimental results. One possible explanation of this is the non-correct analysis of the hydrodynamic conditions of the measurement and, in particular, the assumption of some approximations that may not be necessarily valid in all cases. The introduction of hydrodynamic consideration in the study of interfacial shear rheology has helped to clarify some of the existing discrepancies between measurements performed using different devices, thus allowing one to establish clearly the viscosity range in which different techniques can operate with enough sensitivity for determining the interfacial shear viscosity. This review puts in perspective the most recent developments on the studies of the interfacial shear rheology of fluid/fluid interfaces, analyzing the strength and weakness of the different approaches.

Keywords: interfaces, shear rheology, micro-rheology, macro-rheology, hydrodynamics

Research highlights

- Determination of interfacial shear viscosity presents implications in many fields.
- Many techniques accessible to determine interfacial shear viscosity
- Physically reliable viscosities are only obtained using detailed hydrodynamic analysis
- Combining micro- and macro-rheological techniques is possible to cover a broad range of interfacial viscosities.

1. Introduction

Rheology studies the way in which materials deform and flow as response to mechanical stresses [1]. At low frequency, most liquids show viscous flow with negligible shear elasticity modulus. On the other hand, the flow in solids is completely hindered, and the elastic modulus characterizes completely their mechanical behavior. The scenario becomes more puzzling when complex fluids, such as concentrated polymer solutions, gels, colloidal dispersions, etc., are considered because they exhibit a broad variety of different behaviors, in which both the loss and the elastic moduli contribute to the deformation and flow, the so-called viscoelastic behavior, typical of soft matter. It is important to notice that the rheological behavior of materials is coupled to their microstructure, and in many cases the flow field modifies it, thus making it very difficult to build a complete theory to describe the rheology of the system. [2*, 3].

In contrast with bulk or 3D systems, when surface-active species confined at fluid/fluid interfaces (quasi-2D systems) are considered, viscoelasticity is ubiquitous. The understanding of the response of such systems against mechanical perturbations is important because of the relevance of the interfacial dynamics in many technological and scientific areas, ranging from living systems and new materials to environmental science, and from microfluidics to personal care products and food technology [4**,5]. However, the study of the interfacial viscoelasticity remains in some cases challenging, especially due to the small thickness of the interface which makes it difficult to decouple the interfacial response from that corresponding to the adjacent bulk fluids. Therefore, the interfacial rheological characterization is based on the development of tools enabling for the study of the response to small surface stresses which appear isolated of the bulk stresses. In recent years, many studies have dealt with the understanding of the response of interfacial systems either to dilational or to shear deformations [4**, 6*, 7, 8*, 9, [10] 11].

Ultrathin films, such as monolayers at fluid/fluid interfaces, present four main deformation modes which can be classified in two groups: in-plane and out-of-plane deformations. Among the former one are included dilation that involves the study of the response of the interface to changes of the interfacial area, with the interfacial shape remaining constant, and shear which is related to the response of the interface to changes in its shape, without modification of the interfacial area. On the other side, the main out-of-plane modes include bending and torsion. In general, the different modes appear coupled, which frequently complicates extracting the values of the real and imaginary components of the corresponding viscoelastic moduli. However, the coupling may also have advantages, e.g. for obtaining dilational moduli using experimental techniques that are sensitive to the capillary waves [12, 13]. Furthermore, there is coupling between interfacial modes and mechanical properties of the adjacent phases [14] or their structure, e.g. the thickness of the double layer beneath the charged monolayers [15]. Nevertheless, flat horizontal interfaces are the configuration of choice for shear rheology experiments because they ensure that the influence of the other three modes of deformation is negligible. Consequently, in the following it is assumed flat horizontal interfaces.

Shear rheology is focused on the effect of in-plane shape changes of a flat interface due to the application of a controlled shear stress, keeping constant the interfacial area. This type of experiments provides information of the lateral cohesion of the interfacial layers. The shear viscoelastic modulus is a frequency dependent complex magnitude, and gives information on the storage [shear elastic modulus $G'(\omega)$] and the loss [shear viscous modulus $G''(\omega)$] of energy during the deformation [7].

In recent years, many aspects related to the equilibrium properties and the structure of interfacial layers have been unravelled. However, less attention has been paid to the understanding of the mechanical properties of such systems, especially to the interfacial shear rheology. Interfacial shear viscosity is generally difficult to measure, especially for small

molecules,,remaining below the precision of most instruments unless the interfacial layer is largely condensed. For instance,pentadecanoic acid monolayers at the water/vapour interface (PDA) show viscosity values below 10^{-9} N·s·m^{-1} in the expanded liquid state [16*]. Thus, its accurate determination becomes difficult in many cases. Moreover, the interfacial contribution is frequently smaller, or at most comparable, to those corresponding to the adjacent bulk phases. This is particularly important when the length scale of the probe used for the measurement is much larger than the thickness of the interface [4]. Recently, with the development of the micro-rheological techniques [17**] and the proposal of a new magnetic rod interfacial rheometer driven by a mobile magnetic trap [18**], it has been possible to enlarge the range of viscosities accessible on the studies of shear rheology, by enhancing their experimentally accessible range. Both active and passive micro-rheological techniques have further extended the range to ultralow surface shear viscosities [2*]. This review is devoted to the study of the shear rheology of fluid interfaces. For this purpose, first a general discussion on the physical bases governing the interfacial shear response is included, paying special attention to the different methods which provide information about the interfacial viscoelastic shear modulus. Then, a discussion on the discrepancies existing between the results obtained for different interfaces using macro- and micro-rheological methods is included. To finish the current state of the study of interfacial shear rheology is discussed, focusing the interest on the most recent advancements for enhancing the sensitivity on the determination of the interfacial viscoelastic shear properties.

2. Physical bases of interfacial shear rheology studies

It can be assumed that interfacial rheology is the reduction of bulk rheology to systems confined at fluid/fluid interfaces. Therefore, the interfacial shear deformation is confined

within the xy plane [6, 7, 8]. This spatial confinement constrains the application of the 3D rheology concepts for describing the shear response of fluid/fluid interfaces, making it necessary to take into account three different aspects: (i) the correct analysis of the shear response requires a symmetric interfacial stress tensor, (ii) the coupling between the response of the interface and the adjacent bulk phases must be considered for the data analysis, and (iii) the deformation must be carried out at constant area avoiding radial flows [12, 19]. Thus, considering deformations within the interfacial plane (xy) it is possible to define an interfacial shear viscoelasticity G as a proportionality constant between the applied deformation or strain (u_{xy}) and the shear stress (σ_{xy}). When solid-like films are considered a mainly elastic (Hookean) behaviour is found which is characterized by $\sigma_{xy} = Gu_{xy}$. For ideal fluid like films, pure viscous (Newtonian) behaviour characterized by $\sigma_{xy} = \eta_s \, du_{xy}/dt$ is found. In general,

$$G(\omega) = G'(\omega) - i\omega\eta_s(\omega) \equiv G'(\omega) - iG''(\omega). \quad (1)$$

As abovementioned interfacial shear viscoelasticity is associated with the interactions appearing between the surface active compounds, and such interactions affect to the values of the viscoelastic parameters (G, η_s). In general, attractive interactions lead to the increase of both G and η_s in homogeneous interfacial systems. This is because the overcoming of the attractive interactions requires applying some energy so that the molecules can flow within the interface. It is important to note that most interfacial layers show the so-called viscoelastic shear response which is defined by the complex shear modulus.

3. Foundations of interfacial shear rheology

Most of the studies on interfacial shear rheology are based on the measurement of the effect of a 2D complex fluid on the motion of a probe dragged at the interface following a Brownian

motion or a controllable and measurable pattern. Therefore, an accurate determination of the interfacial rheological properties relies on the use of probes sensing small interfacial perturbations while minimizing the role of bulk contributions in their response.

Several techniques relying on the use of probes with different shapes and sizes have been developed for studying the response of interfaces against shear deformation. These techniques can be divided in two different groups: indirect and direct methods. The former ones are based on the measure of the velocity profiles, or more properly the mean square displacement $\left\langle \Delta r^2(t) \right\rangle$, of inert particles embedded at the interface. On the other hand, direct methods rely on the determination of the displacement or motion of a probe placed directly at the interface, on which an external force is imposed.

3.1. Macro-rheological methods

Conventional rotational rheometers traditionally used in 3D rheology, have been adapted for interfacial measurements with bicone [20] or ring [21] fixtures, and are probably the most extended type of instruments used for the characterization of the shear rheology of interfacial layers [22, 23]. Other widespread techniques for the rheological characterization of interfaces are the deep-channel surface viscometers [24, 25] and the magnetic rod rheometers (ISR) [26, 27**, 28]. Furthermore, X-ray photo correlation spectroscopy (XPCS) also provides information about the mechanical moduli comparable to those obtained using conventional rheometers [29, 30].

Even though the measurement procedure of direct methods can be considered simple, it is necessary to take into consideration different hydrodynamics aspects to obtain proper viscosity values. The seminal works on the application of hydrodynamics considerations to different measurement configurations published by Goodrich et al. [31, 32] almost fifty years ago. This is currently tackled by means of flow field based raw data processing methods. Restricting the

discussion to the case of an oscillatory motion of the probe (i. e. oscillatory shear stress), from the seminal work by Reynaert et al. [33] several applications of similar methods to different macro-rheological systems have seen the light. They have been adapted, for instance, to the double wall-ring rotational rheometer [21], the Helmholtz coil driven ISR with magnetic microwire probes [16*, 26], the magnetic trap ISR [18**], and, very recently, the bicone rotational rheometer [34**]. These applications share some common features. In the following, the most fundamental aspects of this methodology for the case of the magnetic needle ISR (being a the needle radius) and the bicone (being R the measurement cell radius) will be discussed.

First, it is necessary to provide the definition for the simplest flow configuration which suits the symmetry of the rheometer geometry, and that may be a fair representation for the real stationary flow configuration provided no secondary instabilities occur. For instance, in both the classic and the magnetic trap driven ISRs at a water/vapor interface, the needle is supposed to move along the symmetry axis of a half cylinder creating a flow that has only one relevant velocity component, parallel to the symmetry axis and depending only on the radial and azimuthal coordinates in the plane normal to the symmetry axis, so that the fluid flow in the bulk is represented as a two-dimensional problem. Similarly, the fluid velocity has only azimuthal component in the bicone geometry, where a cylindrical coordinates system is considered (see Figure 1) [35].

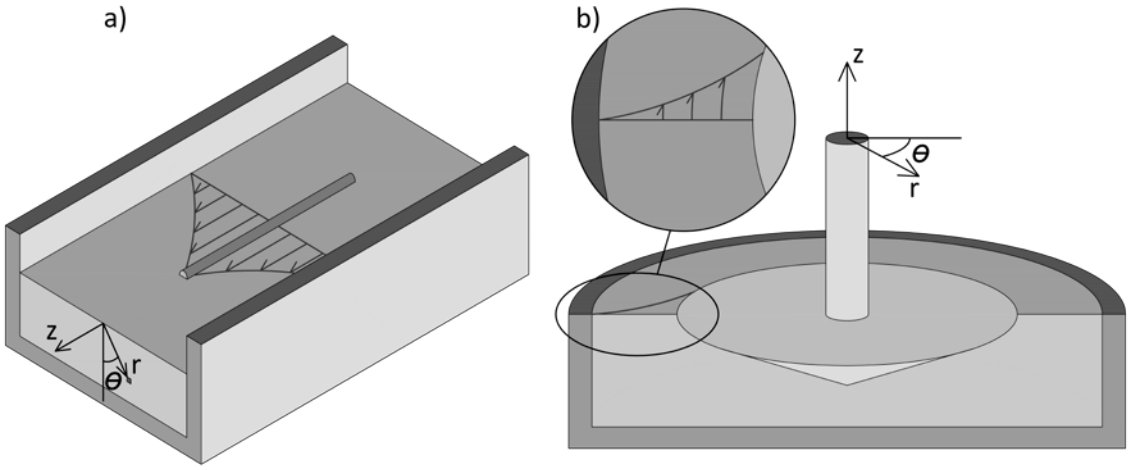

Figure 1 Scheme of the geometries and the coordinates system used in the equations corresponding to the magnetic needle ISR (a) and the bicone (b). The non-linear velocity profiles at the interface that may appear under certain conditions are shown. Extracted from Ref. [35], Creative Commons 4.0.

Second, one has to express the velocity of any fluid element as a function of the probe velocity (which is the experimentally measured observable), so that the fluid velocity for the ISR and the bicone geometries are, respectively

$$v_z(r,\theta,t) = g^*(r,\theta)v_z^{(p)} \tag{2}$$

and

$$v_\theta(r,z,t) = g^*(r,z)v_\theta^{(p)}, \tag{3}$$

where the superscript (p) is referred to the probe velocity, and g^* is a complex function whose real and imaginary parts represent the in-phase and out-of-phase components of the fluid element velocity with respect to the probe velocity, respectively.

Third, it is necessary to write down the Navier–Stokes equations particularized for the 2D problem. Assuming that, first, the probe displacement is periodic with angular frequency ω, and second, after all transients have decayed the fluid velocity is periodic with the same frequency, the Navier-Stokes equation for the ISR and the bicone geometries reads, respectively

$$\frac{\partial^2 g^*(p,\theta)}{\partial p^2}+\frac{\partial^2 g^*(p,\theta)}{\partial \theta^2}=i\,\mathrm{Re}\,e^{2p}g^*(p,\theta), \tag{4}$$

where $p=\ln\left(\frac{r}{a}\right)$, and

$$\frac{\partial^2 g^*(r',z')}{\partial r'^2}+\frac{\partial^2 g^*(r',z')}{\partial z'^2}+\frac{1}{r'}\frac{\partial\, g^*(r',z')}{\partial r'}-\frac{g^*(r',z')}{r'^2}=i\,\mathrm{Re}\,g^*(r',z')\ , \tag{5}$$

where $r'=\frac{r}{R}$ and $z'=\frac{z}{R}$.

The Reynolds number takes, in both cases, the form $\mathrm{Re}=\rho\omega l^2/\eta$ where l equals a for the ISR and R for the bicone, with ρ and η being the density and viscosity of the fluid, respectively, and ω being the deformation frequency. The appropriate boundary conditions [33] must be considered: i) no slip at the measurement cell and probe surfaces, and ii) the Boussinesq-Scriven boundary condition, reflecting continuity of stresses, at the free interface, defined for the ISR and the bicone geometries as

$$Bo^* e^{-p}\left[\left(\frac{\partial^2 g^*(p,\theta)}{\partial p^2}\right)\bigg|_{\theta=\pi/2}-\left(\frac{\partial g^*(p,\theta)}{\partial p}\right)\bigg|_{\theta=\pi/2}\right]-\left(\frac{\partial g^*(p,\theta)}{\partial \theta}\right)\bigg|_{\theta=\pi/2}=0, \tag{6}$$

$$Bo^*\frac{\partial}{\partial r'}\left(\frac{1}{r'}\frac{\partial}{\partial r'}\left(r'g^*(r',z')\right)\right)\bigg|_{R_1'<r'<1,\ z'=h'}-\left(\frac{\partial g^*(r',z')}{\partial z'}\right)\bigg|_{R_1'<r'<1,\ z'=h'}=0, \tag{7}$$

where $R_1' = R_1 / R$ and $h' = h / R$ are the normalized conical bob radius and measurement cell height. This latter is defined as the distance between the bicone rim and the surface of the cup.. The complex Boussinesq number, Bo^* appears defined as

$$Bo^* = \frac{\eta_s^*}{a\eta}, \tag{8}$$

where η_s^* and η are the viscosities of the surface and the subphase, respectively and with the parameter a ranging from the milimeter scale in rotational rheometers (where a is the bicone radius) down to several microns for the case of the magnetic microrod and microwire rheometers (where a is the magnetic rod radius) [16*].

Fourth, it must write down the force, or torque, balance equations for the system under consideration, including the drag components corresponding to the subphase and the interface expressed by means of the appropriate stress tensor components. This equation finally yields an equation for the complex force-position, or torque-angular displacement, amplitude ratio in which terms representing inertia, interface and subphase drags, and eventually a probe confining force, appear

$$AR^* = i2L\omega\eta Bo^* \left(-\frac{\partial g^*(p,\theta)}{\partial p} \right)\Bigg|_{p=0,\ \theta=\pi/2} + i2L\omega\eta \int_0^{\pi/2} \left(-\frac{\partial g^*(p,\theta)}{\partial p} \right)\Bigg|_{p=0} d\theta + k - m\omega^2, \tag{9}$$

$$AR^* = i2\pi R_1 \omega\eta \left[\int_0^{R_1} r^2 \left(\frac{\partial g^*(r,z)}{\partial z} \right)\Bigg|_{z=h} dr - R_1 R Bo^* \left(R_1 \left(\frac{\partial g^*(r,z)}{\partial r} \right)\Bigg|_{r=R_1,\ z=h} - 1 \right) \right] - I\omega^2, \tag{10}$$

where L and m are the needle length and mass, respectively, k represents the confining force of the ISR (this parameter is null in the magnetic trap ISR), and I is the conical bob moment of inertia.

The experiments consist in the measurement of AR^*, that we will refer to as $AR^*_{\exp}$. The calculation of the dynamic surface moduli is usually performed through the iterative procedure

$$Bo^{*\{i+1\}} = \frac{AR^*_{\exp}}{AR^{*\{i\}}_{calc}} Bo^{*\{i\}}, \tag{11}$$

where i denotes the iteration cycle. Inserting a reasonable seed value for Bo^* allows for computing the flow field, obtaining the subphase and interface drags, and, finally a new value for the calculated amplitude ratio, AR^*_{calc}, which can be used, together with the experimental complex amplitude ratio, AR^*_{exp}, to build up an iterative process that, upon convergence, yields the value of the complex Boussinesq number that yields a complex amplitude ratio equal to the experimental one. Finally, the complex viscosity can be obtained through the expression

$$\eta^*_s = Bo^* a\eta . \tag{12}$$

Some caveats are in order here. First, this scheme considers constant values of the complex viscosity. Hence it cannot accurately represent experimental situations in which a strongly shear rate viscosity dependence and locally strong velocity gradients may result in spatially inhomogeneous complex viscosity. Second, the iterative process is not guaranteed to be convergent. Third, it is not guaranteed that, in case of convergence, the solution of the iterative process is unique, i.e. multiplicity of solutions cannot be ruled out. In some sense, in Eq. 11, together with Navier-Stokes equations, the boundary conditions and the force, or torque, balance equations, can be seen as a two-dimensional nonlinear iterative map, and there is not a theorem proving that the existence of single stable fixed point in this point. Therefore, a critical evaluation of the results obtained through such procedures is mandatory.

In the case of the magnetic trap ISR, it has been shown that by means of an adequate treatment of the hydrodynamic flow field at, both, the interface and the bulk, in the spirit of [21, 26, 33],

and using microwire probes the instrument is capable of a 10^{-9} N/m resolution in dynamic moduli, while using KSV-Nima commercial magnetic needles the instrument can accurately measure dynamic moduli up to 10^{-1} N/m [16*, 18**].

An appropriate account for the contributions of the interface and the subphase drags, as well as for the inertia terms, is crucial for determining the range of viscosities that a given rheometer can measure with enough precision. For the sake of example, Figure 2 shows the corresponding results for the monolayer of pentadecanoic acid, PDA, in measurements performed at constant frequency. It is obvious that only for the surface pressure ($\Pi = \gamma_0 - \gamma$ with γ_0 and γ being the surface tensions of the bare interface and of the interface with a monolayer, respectively) range for which the surface contribution is higher than the subphase one, the rheometer is suitable. It worth remarking that the inertia terms are constant, with the one corresponding to the microwire being much lower that for the commertial needle, as expected. The vertical lines indicate the surface pressure values at which the surface drag equals the subphase drag for, both, the microwire (solid symbols) and the commertial needle (empty symbols).

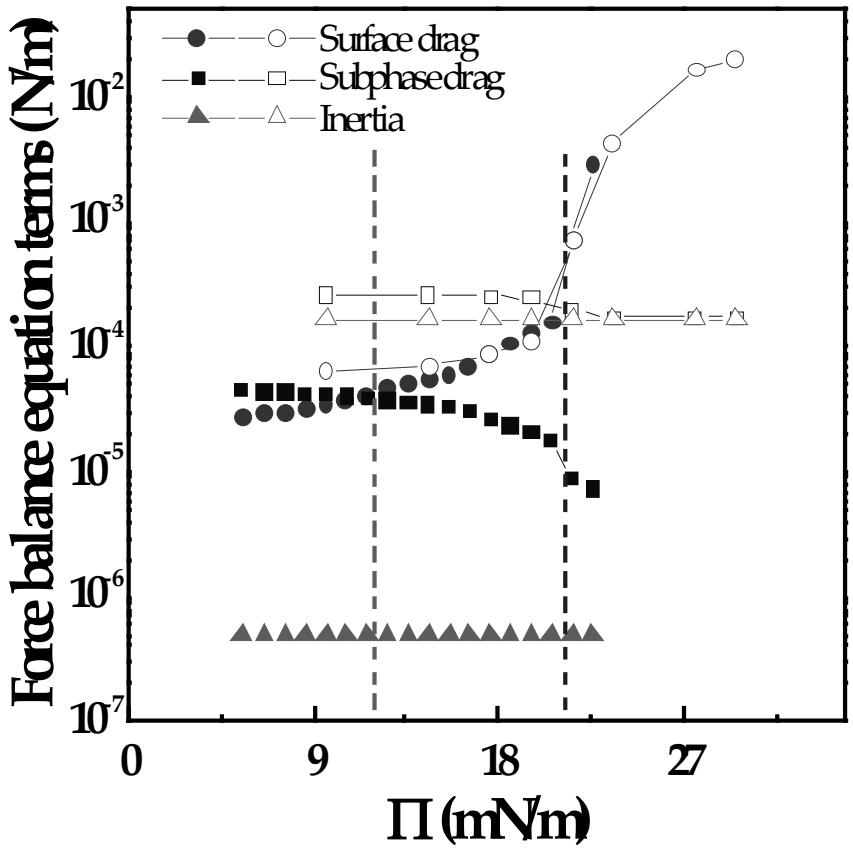

283

284 Figure 2. Dependences of the force balance equation terms on the surface pressure calculated
285 for PDA monolayers spread at the water/vapor interface using the conventional ISR with two
286 different probes, namely microwire (solid symbols) and KSV-Nima commercial magnetic
287 needle (empty symbols). The vertical lines indicate the surface pressure values at which the
288 surface drag equals the subphase drag for, both, the microwire (solid symbols) and the
289 commertial needle (empty symbols).

290

291 **3.2. Micro-rheological methods**

292 In recent years, microrheological techniques have undergone a spectacular development on the
293 study of the shear response of fluid interfaces. Among these techniques passive techniques
294 such as particle tracking (PT) [17**] and active ones such as ferromagnetic microbutton are

included [36]. Both approaches rely on tracking the displacement of a micro-sized probes confined at the interface. The probe displacement at the interface can be autonomous (passive methods) or stimulated by external fields such as magnetic ones (active methods). In PT experiments the thermal movement of a probe particle confined in the viscous or viscoelastic interface is track by using a fast optical microscopy technique. Usually one follows the set of individual particles present in the view field, frequently in the range 200 – 500 particles, and calculate the single-particle, and the relative (particle-particle), mean square displacement (MSD, $<\Delta r^2(t)>$). In general the single particle MSD can be written as

$$<\Delta r^2(t)>= 2dDt^{\alpha}\,, \tag{13}$$

where D is the diffusion coefficient that can be connected to the hydrodynamic friction coefficient through the Einstein relation, $D = k_B T / f$, where k_B is the Boltzmann´s constant, T the absolute temperature and *f* the friction coefficient exerted on the probe particle, and d is a parameter providing information about the dimensionality within the translational motion occurs. For the case of interfaces d assume the value of 2. The exponent α provides information of the nature of the particle motion. For the case of a purely viscous interface, α = 1 and the particle motion at the interface becomes purely viscous, thus $<\Delta r^2(t)>$ for pure viscous interfaces reads

$$<\Delta r^2(t)>= 4Dt\,. \tag{14}$$

For interfaces with high viscosity α < 1, leading to a subdiffusive motion. For heterogeneous interfaces, the above definition of the MSD leads to erroneous results, and it is necessary to define the relative mean square displacement ($<\Delta r_{rel}^2(t)>$). This accounts for the fluctuations of pairs of particles separated a R_{ij} distance for all the possible values of R_{ij}. For the determination of the relative MSD, first it is necessary to calculate the temporal evolution of

the displacement vector of each particle, and then an average of the displacement vectors for the ensemble is calculated

$$D_{\alpha,\beta}(r,\tau) = \left\langle \Delta r_{\alpha}^{i}(r,\tau)\Delta r_{\beta}^{j}(r,\tau)\delta\left[r - R_{ij}(t)\right]\right\rangle_{i\neq j,t}, \quad (15)$$

$$\Delta r_{\alpha,\beta}^{i,j}(r,\tau) = r_{\alpha,\beta}^{i,j}(t+\tau) - r_{\alpha,\beta}^{i,j}(t), \quad (16)$$

where i and j are labels for two different particles, and α and β represent the coordinate axes. τ represents the lag time. For the case of purely viscous interface, the relative mean square displacements can be written as $<\Delta r_{rel}^{2}(t)>=8Dt$ .Hydrodynamic calculations of f by Danov [37, 38, 39] and Fischer [40] can be used to estimate interfacial viscosities from the 2D diffusion coefficients. In the case of viscoelastic interfaces the MSD is not any more linear with time. In fact, Figure 3 schematizes the expected MSD variation for the simplest viscoelastic models used in 3D rheology.

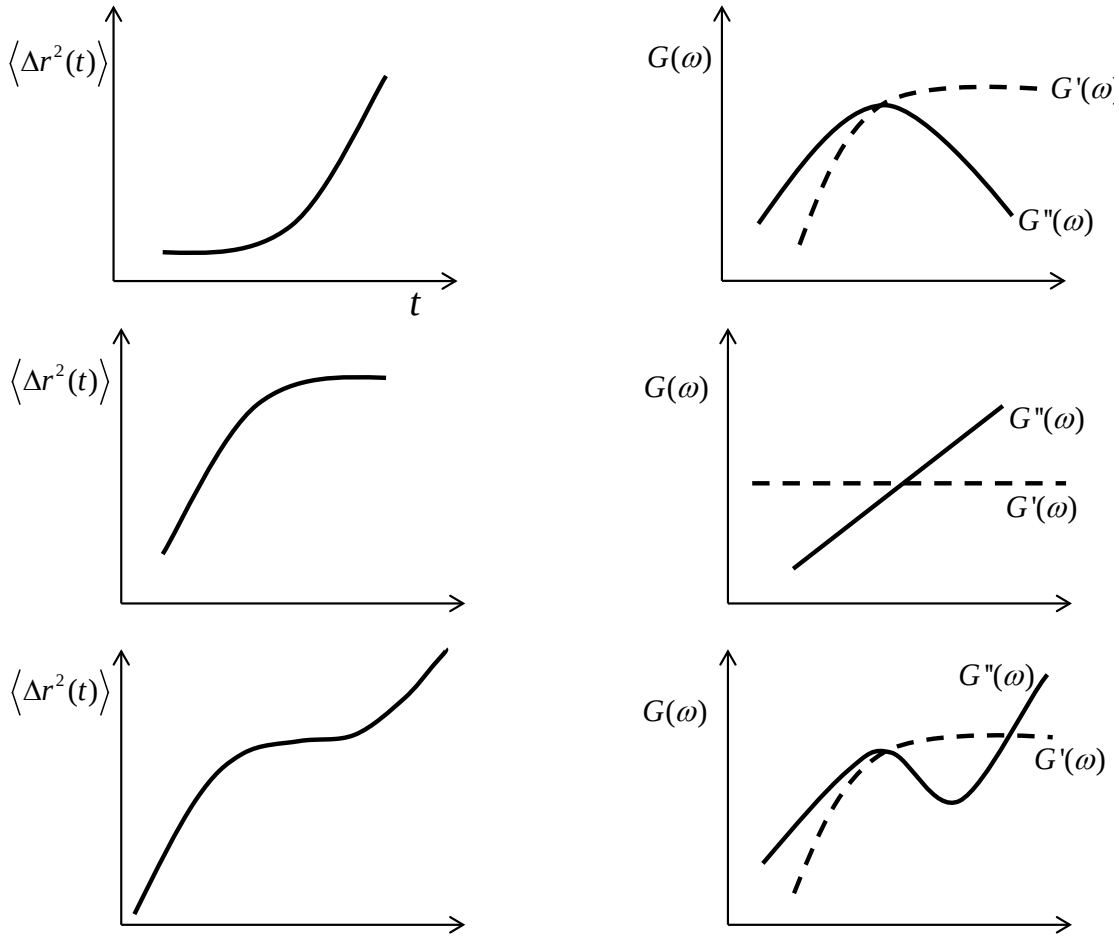

329

330 Figure 3. For the simplest viscoelastic models: MSD dependences on time and frequency
331 dependences of $G'(\omega)$ (dashed line) and $G''(\omega)$ (solid line).

332

333 A different approach in PT is the use of the generalized Stokes-Einstein equation, originally
334 devised for 3D systems, to extract directly from the MSD the interfacial shear viscous and
335 elastic moduli. It is worth mentioning that the description of the experimental results in terms
336 of the viscoelastic models shown in Figure 3 (Maxwell, Kelvin-Voigt, Jeffrey) present a semi-
337 empirical character [41]. In addition to the above models, a four one, the so-called modified
338 Jeffrey model must be also taken into account. This latter model is able to provide a description

of the slope of the viscoelastic modulus in the low shear rate region, which is not well described using any of the other models [42].

3.3. Discrepancies between macro-rheology and micro-rheology

Macro- and microrheological techniques provide information related to the same properties, however when the rheology of interfacial layers is considered very large discrepancies are found in the obtained results using different methods [43*]. This is very different to the situation found for bulk measurements in which good agreement between macro- and micro-rheology has been found [44**].

For some time, the source of such discrepancies remained unexplained. However, recent developments on the characterization of the shear response of interfacial film allow explaining these differences on the bases of two different issues: (i) incorrect definition of the flow field [34**], and (ii) no inclusion of the drag of the bulk phases in the description of the probe motion [45]. The solution of the problems associated with the correct analysis of the flow field is not trivial and requires complex hydrodynamics considerations [16*, 18**, 21, 26, 33]. Recalling to the dimensionless Boussinesq number (Eq. (2)) it is possible to weight the relative importance of the interfacial and subphase contributions in the shear response. This provides information about the sensitivity of the measurement geometries for determining the shear response [46]. Assuming a drag on the rheological probe exerted along the contact perimeter, P_c, a bulk contribution occurring along the contact area, A_c, and similar characteristic velocity decay lengths in both, the interface and the subphase, the Boussinesq number (Eq. (8)) can be rewritten as follows

$$Bo^* = \frac{\eta_s^* \frac{V}{L_I} P_c}{\eta \frac{V}{L_S} A_c} = \frac{\eta_s^* L_S P_c}{\eta L_I A_c} = \frac{\eta_s^*}{\eta a}, \tag{17}$$

where V indicates the characteristic velocity of the probe, and L_I and L_S represent the characteristic length scales at which the velocity decays at the interface and in the subphase, respectively. For $\left|Bo^*\right|$ >> 1, the surface stresses govern the probe response whereas for $\left|Bo^*\right|$ << 1 the stresses associated with the adjacent bulk phases are the most important contributions and, therefore, the chosen probe is not suitable for interfacial studies. On the bases of the above discussion the maximum sensitivity in the rheological measurements is achieved when the contact area of the probe with the subphase is minimal. The above discussion evidences clearly the importance of a careful hydrodynamic analysis of the system to discriminate between the role of the interfacial contribution and those of the adjacent bulk phases. Table 1 reports characteristic values of $\left|Bo^*\right|$ for common probes used in the determination of the interfacial shear viscosity.

Table 1. Characteristic values of $\left|Bo^*\right|$ for different probes used in the determination of the interfacial shear viscosity.

Probe	**Size (mm)**	$\left\|Bo^*\right\|$ **(η_s^* = 10^{-8} N.s/m)**	$\left\|Bo^*\right\|$ **(η_s^* = 10^{-4} N.s/m)**
Bicone	30	0.00033	3.3
DWR	1	0.01	100
KSV-Nima rod	0.4	0.025	250
Microbutton	0.02	0.5	5000
Microwire	0.02	0.5	5000
Colloidal particle	0.001	10	100000

Recently, it has been shown that the discrepancies between micro- and macro-rheology can be overcome with an adequate treatment of the hydrodynamic flow field, as evidenced the good agreement between measurements carried out with magnetic trap ISR using microwire probes in the previously conflicting range of dynamic moduli in between 10^{-9} and 10^{-6} N/m [16**, 18**]. Figure 4 shows the good agreement between the viscosities obtained using different

macro- and micro-rheological techniques for studies of PDA monolayers spread at the water/vapor interface [18**].

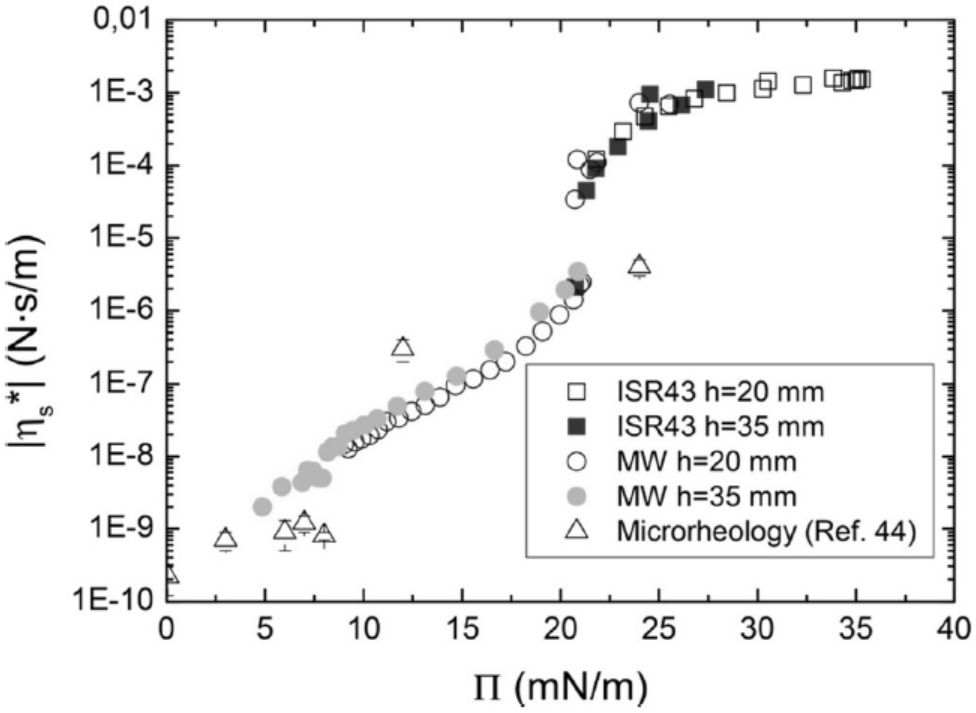

Figure 4. Dependence of the magnitude of the complex interfacial shear viscosity on the surface pressure for PDA monolayers spread at the water/vapor interface as was obtained using different rheological probes: Particle tracking micro-rheology (Δ). Magnetic trap ISR with KSV-Nima commercial magnetic needle at two different distances, h, between the probe and the magnets: 20 mm (□) and 35 mm (■). Magnetic trap ISR with microwire probe at two different distances, h, between the probe and the magnets: 20 mm (○) and 35 mm (●). Reprinted with permission from Ref. [18**]. Copyright 2017, The Society of Rheology.

So far, we have focussed on the analysis of the most fundamental bases underlying the study of the interfacial response against shear deformations. In the following, we will provide a

discussion on the most recent results that have contributed to solve the main problems of this type of studies.

4. Experimental results

The rheological characterization of 3D materials using both micro- and macro-rheological techniques presents in most cases a reasonable good agreement within the combined experimental precision provided using different techniques [47]. However, the situation becomes more complex when studies on system confined at interfaces are considered. In particular, differences have been found between the results obtained using conventional rheometers and micro-rheological techniques.

Maestro et al. [43*] studied Langmuir monolayers of poly(tert-butyl acrylate), PtBA monolayers spread at the water/vapor interface by means of, both, a rotational rheometer with a bicone fixture and particle tracking microrheology. The authors found qualitative agreement on the dependences of the shear viscosity on the surface density and the chain length obtained using the conventional rheometer and the micro-rheological technique. However, they reported differences on the measured shear viscosity of about three orders of magnitude between particle tracking and macro-rheometer measurements. Figure 5 shows the dependence of η_s^* on the surface concentration and the number of monomer in the chain for PtBA monolayers spread at the water/vapor interface [43*, 48].

The discrepancies between the results obtained using a conventional rheometer and particle tracking for polymer monolayers were firstly ascribed to two different possible reasons, which were related to the particle-tracking method. The first one was related to possible incorrect assumptions in the models used for obtaining the value of η_s^* from the diffusion coefficient of

the particles at the fluid interface. The second reason was related to the possible appearance of heterogeneities in the polymer monolayer due to the formation of a depletion layer around the particles, which reduces the effective polymer concentration in the surrounding of the particle and thus the value obtained from particle-tracking experiments corresponds to the η_s^* of a less dense state than that of the monolayer. However, Maestro et al. [43*] performed *ad hoc* experiments and calculations evidencing that neither the hydrodynamic model used for the analysis of the experimental results nor the appearance of specific interactions between the particles and the polymer explained the discrepancies. The authors suggested that the discrepancies between macro- and micro-rheological techniques arose from the different sensitivity of the used probe for measuring the interfacial properties.

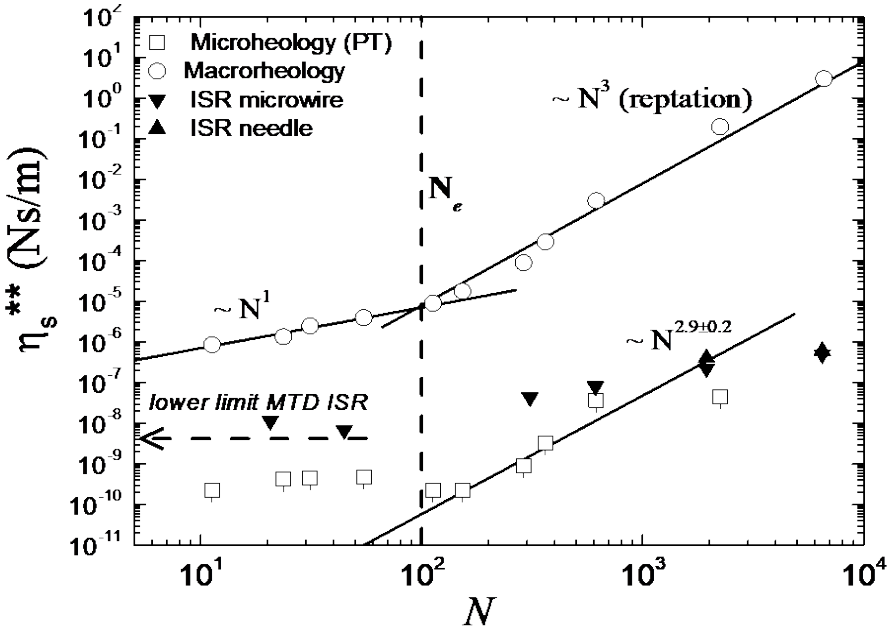

Figure 5. Number of monomer, N, dependences of η_s^* obtained using particle tracking micro-rheology (□), an interfacial oscillatory rheometer (○), interfacial shear rheometer with magnetic microwire probe (▼) and interfacial shear rheometer with needle probe (▲) for Langmuir monolayers of PtBA of different average molecular weights spread at the water/vapor interface. Particle tracking micro-rheology and interfacial oscillatory rheometer

data obtained by are adapted from Ref. [43*] with permission of The Royal Society of Chemistry and data obtained using interfacial shear rheometer with microwire and needle probes are adapted from Ref. [48].

Recently, Samaniuk and Vermant [49] tried to shed light on the above discrepancies for monolayers of PtBA at the water/vapor interface and carried out microscopy images of the obtained monolayers. Their results evidenced the presence of heterogeneities in the monolayers which they considered as a limiting factor for the homogeneous distribution of particles within the interface. The authors suggested that such heterogeneities precluded the micro-rheological study of the shear viscosity of PtBA monolayers. In order to clarify this point Brewster Angle Microscopy (BAM) and ellipsometry studies of PtBA monolayers spread at water/vapor interface prepared following the same procedure used in Ref. [43*] have been carried out. BAM images of PtBA monolayers showed a perfectly homogeneous interface without any presence of heterogeneous structures (see Figure 6). Furthermore, the average film thickness obtained using ellipsometry remains in all the cases in values typical to those expected for a molecular film.

Thus, the presence of aggregates at the interface found by Samaniuk and Vermant [49] does not correspond to the PtBA experiments described in Ref. [43*]. As a complementary evidence of the BAM sensitivity to detect interfacial heterogeneities see, for instance, Figure 6c, in which interfacial heterogeneities were found. These images correspond to a similar PtBA sample that was stored in a container with a polystyrene cap instead of the usual glass cap. The dissolution of the polystyrene of the cap can lead to sample contamination during preparation and storage, which can lead to the appearance of heterogeneities at the interface.

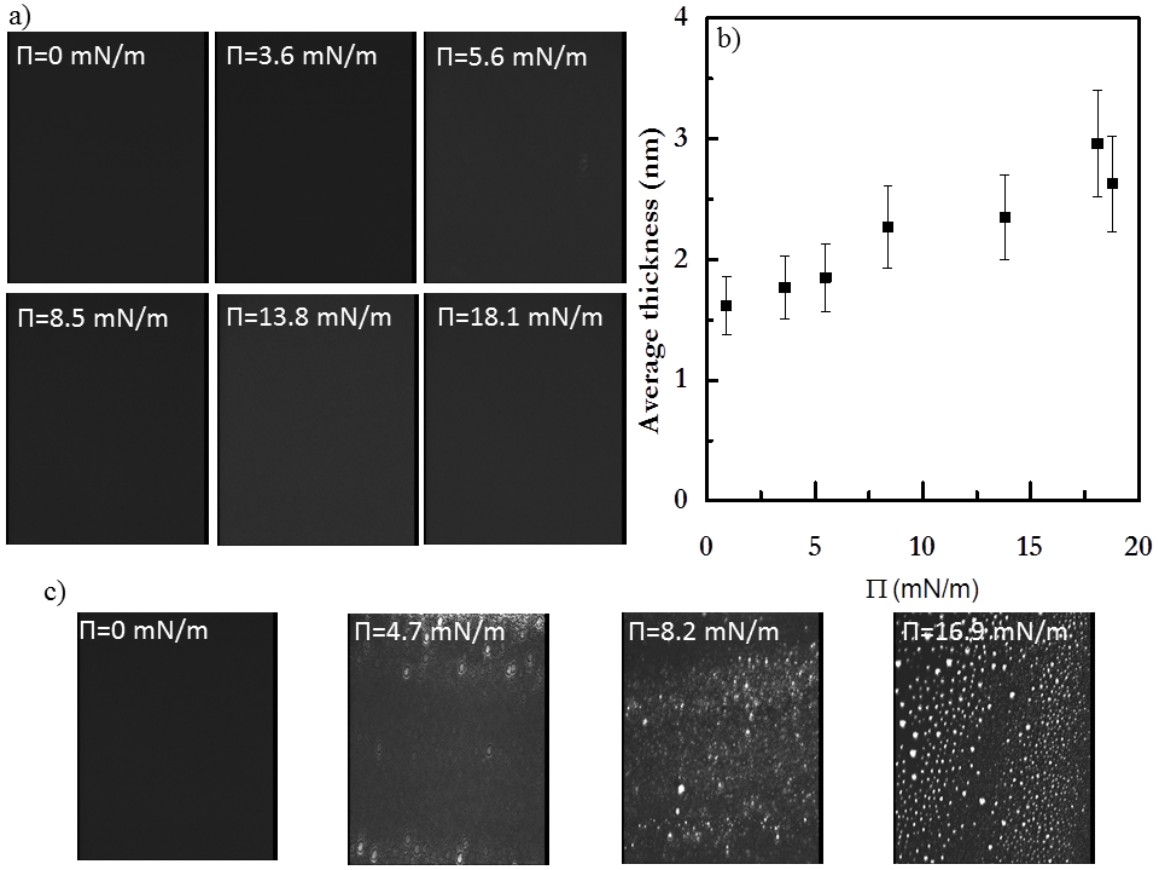

455

456 Figure 6. (a) BAM images (544 x 544 μm^2) for Langmuir monolayers of PtBA (average
457 molecular weight 7.5 kDa) spread at the water/vapor interface. (b) Average thickness of a
458 Langmuir monolayers of PtBA (average molecular weight 7.5 kDa) spread at the water/vapor
459 interface for different surface pressure, $\Pi = \gamma_0 - \gamma$ with γ_0 being the surface tension of the bare
460 water/vapor interface. (c) BAM images (544 x 544 μm^2) for Langmuir monolayers of PtBA
461 (average molecular weight 7.5 kDa) spread at the water/vapor interface. Note the solutions
462 were stored in a container with polystyrene cap which can be the origin of possible
463 contamination.

464

465 To shed light on the discrepancies between micro- and macro-rheology in PtBA, rheological
466 measurements have been performed on similar samples to that studied by Maestro et al. [43*]
467 using an ISR with two probes of different aspect ratio (diamonds and triangles in Figure 5)

468 [48]. A discrepancy (much smaller than the corresponding to the bicone results) is still
469 observed for the low molecular weight (low N) samples. Note that these values of η_s^* are close
470 to the resolution of the ISR ($\left|Bo^*\right| < 1$). However, for larger values of N, the measured
471 interfacial viscosity is higher (which yields to more reliable data) and is in good agreement
472 with the micro-rheological results previously reported by Maestro et al. [43*]. These results
473 suggest that the source of discrepancies is associated with the different sensitivity of the
474 techniques.

475

476 The discussion in the bibliography has been focused so far in the possible failure of micro-
477 rheology techniques. Indeed, in most studies, the possible fail of macro-rheology was not
478 considered. However, there are enough evidences to analyze the issue from a different
479 perspective [50]. If the comparison is restricted to that range in which the involved techniques
480 have enough resolution, a good agreement is shown between experiments performed on: i)
481 PDA using conventional needles and microwires in the ISR [18**], ii) PDA using the ISR and
482 particle tracking (see Figure 4), iii) C24 fatty acid using the ISR and the bicone [34**], and iv)
483 PtBA using the ISR and particle tracking (see Figure 4). These observations call for a careful
484 analysis of first, the range of application of each technique, and second the validity of the
485 normally used approximations in macro-rheology (linearity of velocity decay and simple
486 addition of subphase and interface contributions). Reynaert et al. [33] proposed a successful
487 scheme to properly account for the interfaces and subphase drags in the magnetic rod shear
488 rheometer (ISR) under oscillatory forcing [26]. Similar approach was subsequently applied to
489 the analysis of the rotational rheometer with double wall ring (DWR) fixture [21]. Tajuelo et
490 al. [34**] recently pointed out that the computation of the flow fields of the probe at the
491 interface and the adjacent bulk phases is mandatory to obtain physically reliable η_s^* values in

492 the bicone fixture too. Therefore, the above discussion shows that the problems discussed for
493 PtBA monolayers [43*] might be mainly associated with a non accurate description of the
494 hydrodynamics in the data processing of the measurements performed with the rotational
495 macro-rheometer. In the case of studies of poly(tert-butyl methacrylate) (PtBMA) monolayers,
496 Samaniuk and Vermant [49] discussed the η_s^*, obtained by particle tracking and a magnetic rod
497 interfacial shear rheometer, and found a reasonable dependence η_s^* on the interfacial
498 concentration. However, from their results it was not possible to confirm that micro-rheology
499 and macro-rheology experiments provided the same results. Again, this is because the ranges
500 of viscosities accessible to the different techniques do not overlap, whereas particle tracking
501 allows measuring η_s^* values up to at most 10^{-6} N·s·m^{-1}, the lower measurable limit of a
502 conventional (Helmholtz coil driven) magnetic rod interfacial shear rheometer corresponds at
503 best to η_s^* values of about 10^{-6} N·s·m^{-1}. The problem of the direct comparison between micro-
504 rheological and macro-rheological data due to the sensitivity of the techniques has been
505 recently studied and partially overcome by Tajuelo et al. [16*, 18**]. For this purpose, they
506 performed a detailed analysis of the different terms of the force balance equation involved in
507 the experiment, i.e. drags associated with the interface and adjacent bulk phases and probe
508 inertia. In general, it is assumed that for an accurate determination of the interfacial shear
509 viscosity using a rheological technique, the component of the force balance associated with the
510 interfacial drag must be higher than the other components. As shown in Figure 2 only using
511 microwire probes in the surface pressure range 12 – 21 mN/m would yield realistic values of
512 the interfacial shear viscosity because the interfacial drag component is the most important
513 component to the force balance. In consequence, the direct comparison of the ISR (macro-
514 rheology) and particle tracking (micro-rheology) results requires an enhanced surface to
515 subphase drag ratio, achieved by using smaller and lighter probes than those typically used.

Beyond polymers, the rheological behavior of lipid monolayers has raised big attention in recent years [49, 51, 52, 53, 54, 55], mainly due to the recognized interest of lipids in many phenomena of biological relevance [56*, 57]. Samaniuk and Vermant [49] studied monolayers of 1,2-Dipalmitoyl-sn-glycerol-3-phosphocholine (DPPC) at the water/vapor interface following the same approach used for the studies on PtBMA, and again they found a good agreement between the trend obtained using micro-rheological and macro-rheological techniques. In Ref. [49] the authors expand the sensitivity limit of micro-rheological techniques up to η_s^* values of about 10^{-4} N·s·m^{-1}. Unfortunately, no details were given about the thermodynamic phase in which the studies of the DPPC monolayers were carried out, and this renders difficult to interpret the obtained η_s^* values.

DPPC monolayers at the water/vapor interface were also studied by Kim et al. [58*] using a micro-rheometer based on a magnetic microbutton probe [59, 60]. They studied different regions of the phase diagram of the monolayers. For low surface pressures, DPPC monolayers evidenced a mechanical response against shear reminiscent of line tension mediated elasticity due to the presence of condensed domain in a continuous fluid-like phase. This has been associated with a 2D emulsion-like character of the lipid layer [61]. For the highest surface pressures, the behavior obtained for DPPC monolayers is the one expected for a viscoelastic solid film with both elastic and viscous moduli increasing exponentially with surface pressure. This was explained in terms of the presence of interlocked solid domain at the interface [62]. The η_s^* values obtained using the magnetic microbutton rheometer range from 10^{-7} N·s·m^{-1}, for the lowest surface pressure, to 10^{-5} N·s·m^{-1} for the ordered phase which presents a good qualitative agreement with the results reported by Samaniuk and Vermant [49]. However, no agreement was found with the data by Espinosa et al. [63] obtained using a commercial shear rheometer with biconical bob probe, which evidences again the importance of an accurate

definition of the hydrodynamic conditions affecting the rheological measurements. It is worth mentioning that one of the most important advantages of the use of magnetic microbutton rheometers is that the microstructure of the interface can be observed during the shearing process [64]. The results obtained with the magnetic microbutton rheometer for DPPC monolayers show good agreement with those obtained by Shlomovitz et al. [65] measuring the fluctuations of submerged colloidal tracers as a function of their vertical distance to the interface to calculate the viscoelastic properties of the monolayer [66, 67]. This technique allows one to obtain information by passive micro-rheology even of phases with very low viscosity (~ 10^{-9} N·s·m^{-1}), e.g. liquid expanded phases of lipid monolayers. In principle, the main advantage of the technique used by Shlomovitz et al. [65] is that the passive tracer directly reflects the dynamics at the fluid right below the monolayer. Park et al. [68] using passive (particle tracking) and active (optical tweezers) micro-rheological techniques obtained results in agreement with those by Shlomovitz et al. [65] for DPPC monolayers within the expanded phase.

The magnetic microbutton rheometer has been also used to evaluate the role of the addition of cholesterol in DPPC monolayers [69]. The introduction of cholesterol leads to an exponential-like decrease of the surface viscosity in relation to that of pure DPPC monolayer, reaching this decrease almost two orders of magnitude for mixtures containing 2 wt % of cholesterol [70]. It is worth mentioning that, independently of the cholesterol fraction, an almost linear dependence of the viscosity on the surface pressure was found for monolayers in condensed phases (above 15 mN·m^{-1}). Furthermore, a linear dependence of *G''* on the deformation frequency, ω, was found for the mixtures in the frequency range 0.1 - 10 Hz. Thus, it is possible to define the shear viscosity directly as $\eta_s = G''/\omega$. Similar behaviour to that reported for the effect of cholesterol in pure DPPC monolayers was observed in monolayers of mixtures for lung surfactant replacement. Thus, the decrease of the viscosity is expected to present an

565 important physiological role in the breathing cycle which is associated to decrease of the line
566 tension of the lipid domains within the structure [69]. This modification on the structure is
567 associated with the effect of the introduction of cholesterol in the tilt of the DPPC chains in the
568 monolayer [70,71]. Along this research line, further studies in more complex mixtures
569 including DPPC, cholesterol and a fatty acid (palmitic acid, PA) were carried out using a
570 magnetic microbutton rheometer [72]. This mixture presents the behaviour of a 2D suspension
571 in which pseudo-hard discs are dispersed in a continuous fluid matrix. The low surface
572 pressure region presents a very low viscosity and its rheological response is governed by the
573 drag of the aqueous subphase. The increase of the surface pressure leads to the increase of the
574 size of the discs and the viscosity increases following a power law with surface pressure. For
575 the most condensed phases, a sharp increase of the viscosity (several orders of magnitude) was
576 found depending on the cholesterol content. This is explained for the modification of the
577 conformation of the molecules forming a tilted ordered phase. Ref. [72] also pointed out the
578 important role of the sensitivity of the chosen probe on the determination of the viscosity
579 because high sensitivity is mandatory to assess correctly the influence on the interfacial
580 viscosity of subtle changes of parameters such as composition or temperature, which may lead
581 to misleading interpretations of the experimental findings [73].

582 Active microrheology based on the reorientation of nickel nanorods in a magnetic field was
583 used for studying the phase transitions of monolayers of two different
584 phosphatidylethanolamines, DMPE (1,2-dimyristoyl-sn-glycero-3-phosphoethanolamine) and
585 DLPE (1,2-dilauroyl-sn-glycero-3-phosphoethanolamine) [74]. For disordered monolayers,
586 again, very low shear viscosities were found (about 10^{-9} N·s·m^{-1}) in agreement with those of
587 DPPC [65] and mixtures of DPPC, cholesterol and PA [72]. These viscosities are below the
588 sensitivity of most commercial rheometers, and only very recently have been reached using
589 rheological techniques based in a macroscopic probe by Tajuelo et al. [16**]. The transition on

590 lipid monolayers from disordered phases to ordered phases is evidenced by a jump of almost
591 one order of magnitude in the interfacial shear viscosity, whereas the ordered phases of DMPE
592 and DLPE monolayers show an exponential-like increase of the viscosity with the packing in
593 agreement with the above discussion for mixtures of DPPC and cholesterol [69]. It is worth
594 mentioning that shear viscosities obtained using either the magnetic microbutton micro-
595 rheometer [58, 69, 70] or the analysis of the reorientation of nickel nanorods in a magnetic
596 field [74] are 2 – 3 orders of magnitudes lower than those obtained using conventional
597 oscillatory rheometers [58]. Interestingly, the enhancement of the sensitivity provided by the
598 development of new micro-rheological techniques allows one to perform accurate
599 measurements of η_s^* even for soluble surfactants with very low viscosity (around 10^{-8} N·s·m^{-1}),
600 as was pointed out by Zell et al. [75] in sodium dodecyl sulfate (SDS). Recently Martínez-
601 Pedrero et al. [76] studied β-casein adsorbed films at the water/vapor interface combining
602 particle tracking and home-made magnetic rod interfacial shear rheometer driven by a mobile
603 magnetic trap [18**]. They found good qualitative agreement between the results obtained for
604 their micro-rheological and macro-rheological approaches. Their results point out that the
605 adsorption layers of β-casein at the water/vapor interface present a negligible viscosity until
606 surface pressures about 10 – 15 mN·m^{-1}, and once the layer overcomes that surface pressure
607 the interfacial viscosity increases suddenly with time. This process can be considered a
608 thickening regime governed by the viscous component.

609 Contrary to what happens in the studies of PtBMA and DPPC, Samaniuk and Vermant [49] did
610 not find good agreement in their study of monolayers of a fatty alcohol (hexadecanol) using
611 particle tracking and the magnetic rod interfacial shear rheometer. The disagreement on
612 hexadecanol experiments was not only in magnitude but also in their trend. η_s^* obtained using
613 particle tracking being between 2 and 4 orders of magnitude lower than those obtained using
614 the magnetic rod rheometer. In order to explain such discrepancies, the authors analyzed

615 carefully the hydrodynamic problem, including the role of an extensional component in the
616 flow field through the use of magnetic rods of different aspect ratio. These tests showed a
617 strong dependence of the values obtained for hexadecanol monolayers on the aspect ratio of the
618 magnetic rods, which supports the possible role of a complex flow field. Here again, the
619 complex structure of interfacial layers of hexadecanol might need a careful processing of the
620 hydrodynamic problem to provide accurate viscosity values [77]. Measurements in eicosanol
621 also evidenced discrepancies of about one order of magnitude between micro-rheological [65]
622 and macro-rheological [26] techniques. Shlomovitz et al. [65] proposed two possible
623 explanations for such discrepancies: the first one associated with the possible existence of a
624 frequency dependent i viscous modulus, which was not considered on the comparison between
625 micro-rheological and macro-rheological data. A second reason was associated with the role of
626 the properties of the adjacent bulk phases, which were assumed to be completely viscous for
627 the data analysis. Despite the differences in the absolute values, the trend of the viscosities
628 were correct independently of the measurement techniques, with a mainly viscous behavior at
629 the lowest pressure ($G'' > G'$) and a significant decrease of η_s^* with the surface pressure at the
630 condensed phase [65, 78]. Also experiments carried out using magnetic microbutton
631 microrheometers show qualitative and quantitative agreement with data obtained with the
632 classic (Helmholtz coil driven) ISR in the L_2' phase but only qualitative agreement in the LS
633 phase of eicosanol monolayers [60]. These discrepancies could be explained bearing in mind
634 that the interfacial solidification could be modified by the shear stress. Some years ago, Wu et
635 al. [79], using X-ray reflectivity showed that long-chain alkanes and alcohols surfaces
636 undergone a surface-induced crystallization at a transition temperature higher than the bulk
637 one. This problem has not been analyzed in the above papers, and one might expect higher
638 effect in micro- than in macro-probes.

The interface temperature, T_s, can also play a significant role when comparing results on fatty acid monolayers. A recent study on the surface pressure and T_s dependence of the rheological response of fatty acids [80] demonstrates a strong dependence of the results on T_s. In addition, a proper measurement T_s is far from trivial: the evaporation necessarily decreases T_s with respect to the subphase temperature, so the use of probes such as thermo-couples or PT-100 resistors may lead to incorrect reads of T_s. Clearly, a careful interface temperature control and measurement is mandatory to ensure reproducibility and a proper understanding of the rheological response of these monolayers. The magnetic trap ISR [18**] was used [80] to obtain the phase diagram for fatty acids from 15 to 24 carbon atoms by means of just rheological measurements. The phase diagram presents a remarkable agreement with those previously reported in the literature obtained from structural characterization [81]. The thorough study of the monolayers shear rheology confirmed several already known phenomena such as: i) the existence of a maximum in the viscosity for the L2 phase (liquid condensed phase with nearest neighbor tilt) [82], ii) the small, or negligible, dependence of η_s^* on the surface pressure for the LS phase (superliquid untilted phase) [26, 60], and iii) the increasing of the viscosity with increasing temperature in the LS phase [83], a striking result that was not given much credit because the results were obtained with a slit viscometer that was not considered to yield reliable estimates because the highly condensed LS phase was supposed to have large elastic effects.

Furthermore, they found new interesting rheological features in the behavior of the fatty acid monolayers such as: i), the rheology of, both, the S (solid untilted) phase and the LS phase to be dominated by the viscous modulus, ii) the existence of a viscosity maximum in the L_2' (liquid condensed phase with next nearest neighbor tilt) phase of the fatty acid monolayers close to the transition to the LS phase (suggesting a coexisting zone and, consequently, a first order L_2'-LS transition, iii) the negligible elastic component at the LS phase, which explains

why the results of Ref. [83] on the LS phase viscosity obtained with a viscometer were correct, and, iv) the equivalence between the results of isothermal surface pressure sweeps and isobaric temperature sweeps regarding the anomalous temperature dependence of the viscosity of the LS phase.

Recently, particle tracking have allowed characterizing the effect on the rheological properties of the interfacial collapse of layers of poly N-isopropyl acrylamide (PNIPAm) particles mediated by the increase of temperature. This collapse leads to a change of the interfacial behavior from solid-like to fluid-like [84].

5. Concluding remarks

The discussion in this review concerns to some important issues related to the theoretical description of experiments in interfacial shear rheology and the discrepancies existing between micro-rheology and macro-rheology. It is expected that the range of viscosities accessible for micro-rheological and macro-rheological experiments can differ. However, recent developments have allowed closing the gap existing between the information obtained using micro-rheology and macro-rheology techniques [16*, 17**, 60**]. Figure 7 shows an approximate sensitivity range of the viscosity in which different rheological techniques can operate for the determination of the interfacial shear viscosity. It is worth mentioning that the limitation of the applicability of particle tracking experiments to the low viscosity range is explained assuming that the higher the viscosity the higher the time needed for particles to diffuse distances long enough to provide a good statistics. Thus, the extension of the viscosity range accessible for particle tracking involves enlarging the accessible observation area and/or the velocity of data acquisition and processing using ultra-fast camera and computers,

687 respectively.

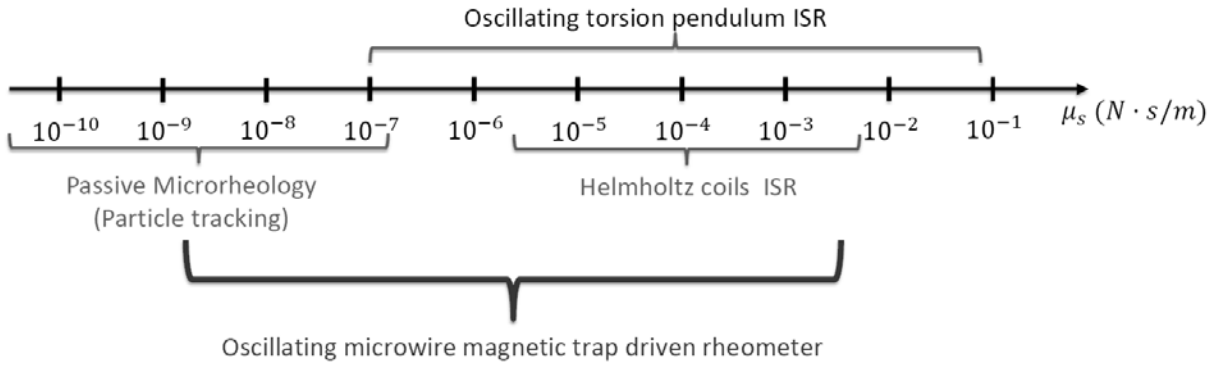

688

689 Figure 7. Approximate sensitivity range for the determination of the interfacial shear viscosity
690 for different rheological techniques.

691

692 It has been extensively discussed along this review the important role of the correct separation
693 of the drags associated with the interface and the adjacent bulk phases, i.e., the correct
694 resolution of the hydrodynamic equation for the specific configuration, in order to obtain
695 physically reliable values of the interfacial viscosity. During long time the studies on shear
696 properties of interfacial layers were carried out exclusively using conventional 3D rotational
697 rheometers with geometries adapted to fulfil the specific requirements of the interfaces.
698 However, in many cases, huge discrepancies appear between different experiments over similar
699 system carried out with such rheometers. This is explained considering the absence of a correct
700 analysis of the flow field of the probe at the interface. This was solved in part by the
701 introduction first of the magnetic rod interfacial shear rheometer (ISR) [26] and then with the
702 development of micro-rheological techniques, both active and passive [16*]. Despite the
703 development of these rheological methods helps to the better understanding of the properties of
704 interfacial films, a small window which was not accessible neither for macro-rheological
705 technique nor for micro-rheological techniques remained unexplored for long time. However,

706 in recent years the development of micro-rheological such as the magnetic microbutton
707 rheometer [64] and macro-rheological techniques, such as the magnetic rod interfacial shear
708 rheometer driven by mobile magnetic trap [18**], have allowed to enlarge the upper limit of
709 viscosity accessible for micro-rheological techniques and the lower limit of macro-rheological
710 techniques, hence closing the gap. Today this leads to the possibility to measure the shear
711 rheological properties of interfacial layers in a broad range of surface viscosities in between 10^{-9}
712 $N \cdot s \cdot m^{-1}$ and several $N \cdot s \cdot m^{-1}$.

713

714 **Acknowledgements**

715 The work of E.G., F.O., and R.G.R. work was funded by MINECO under grant CTQ2016-
716 78895-R and the work of M.A.R., J.M.P and J.T. was funded by MINECO under grants
717 FIS2013-47350-C5-5-R and FIS2017-86007-C3-3-P.

718

719 **References**

[1] Wilkinson DJ. What is Rheology? Eye 2018; 32: 179-183. doi: 10.1038/eye.2017.267.

[2*] Liu W, Wu, C. Rheological Study of Soft Matters: A Review of Microrheology and Microrheometers. Macromol. Chem. Phys. 2017; 219: 1700307. doi: 10.1002/macp.201700307. Comprehensive revision of the application of microrheological techniques to the characterization of the mechanical response of soft matter.

[3] Larson RG. The Structure and Rheology of Complex Fluids. New York, United States of America: Oxford University Press; 1999.

[4**] Fuller GG, Vermant J. Complex Fluid-Fluid Interfaces: Rheology and Structure. Ann. Rev. Chem. Biomol. Eng. 2012; 3: 519-543. doi: 10.1146/annurev-chembioeng-061010-114202. Review discussing some of the most relevant aspects of the rheological behavior of fluid interfaces, providing correlations between the rheological response and the structure of interfacial layers.

[5] Karbaschi M, Lotfi M, Krägel J, Javadi A, Bastani D, Miller R. Rheology of interfacial layers. Curr. Opin. Colloid Interface Sci. 2014; 19: 514-519. doi: 10.1016/j.cocis.2014.08.003.

[6*] Sagis LMC, Fischer P. Nonlinear rheology of complex fluid-fluid interfaces. Curr. Opin. Colloid Interface Sci. 2014; 19: 520-529. doi: 10.1016/j.cocis.2014.09.003. Review analyzing the interfacial response of complex interfaces against mechanical deformations.

[7] Langevin D. Surface shear rheology of monolayers at the surface of wáter. Adv. Colloid Interface Sci. 2014; 207: 121-130. doi: 10.1016/j.cis.2013.10.030.

[8*] Mendoza AJ, Guzmán E, Martínez-Pedrero F, Ritacco H, Rubio RG, Ortega F, Starov VM, Miller R: Particle laden fluid interfaces: Dynamics and Interfacial rheology. Adv. Colloid Interface Sci. 2014; 206: 303-319. doi: 310.1016/j.cis.2013.1010.1010. Study providing a perspective of the current knowledge of the rheology of particle-laden interfaces.

[9] Llamas S, Guzmán E, Akanno A, Fernández-Peña L, Ortega F, Campbell RA, Miller R, Rubio RG. Study of the Liquid/Vapor Interfacial Properties of Concentrated Polyelectrolyte–Surfactant Mixtures Using Surface Tensiometry and Neutron Reflectometry: Equilibrium, Adsorption Kinetics, and Dilational Rheology. J. Phys. Chem. C 2018; 122: 4419-4427. doi: 10.1021/acs.jpcc.7b12457.

[10] Monroy F, Ortega F, Rubio R. Rheology of a miscible polymer blend at the air-water interface. Quasielastic surface light scarrering study and analysis in terms of static and dynamic scaling laws. J. Phys. Chem. B 1999; 103: 2061-2071. doi: 10.1021/jp982548m.

[11] Maestro A, Santini E, Zabiegaj D, Llamas S, Ravera F, Liggieri L, Ortega F, Rubio RG, Guzmán E. Particle and Particle-Surfactant Mixtures at Fluid Interfaces: Assembly, Morphology, and Rheological Description. Adv. Cond. Matt. Phys. 2015; 2015: 917516. doi: 10.1155/2015/917516

[12] Monroy F, Ortega F, Rubio RG, Velarde, MG. Surface rheology, equilibrium and dynamic features at interfaces, with emphasis on efficient tools for probing polymer dynamics at interfaces. Adv Colloid Interface Sci, 2007; 134–135: 175-189. doi: 10.1016/j.cis.2007.04.023.

[13] Langevin D. Light Scattering by Liquid Surfaces and Complementary Techniques. New York, United States of America: Marcel Dekker, Inc., 1992.

[14] Harden JL, Pleiner H, Pincus PA. Hydrodynamic surface modes on concentrated polymer solutions and gels. J. Chem. Phys. 1991; 94: 5208. doi: 10.1063/1.460525.

[15] Miller R, Liggieri L (eds.). Interfacial Rheology. Boca Ratón, United States of America: CRC Press, 2009.

[16*] Tajuelo J, Pastor JM, Martínez-Pedrero F, Vázquez M, Ortega F, Rubio RG, Rubio MA. Magnetic Microwire Probes for the Magnetic Rod Interfacial Stress Rheometer. Langmuir 2015; 31: 1410−1420. doi: 10.1021/la5038316. Work describing a new version of a magnetic needle rheometer with improved sensitivity, allowing for closing the gap between micro-rheological method and macro-rheological methods.

[17**] Ortega F, Ritacco H, Rubio RG. Interfacial microrheology: particle tracking and related techniques. Curr. Opin. Colloid Interface Sci. 2010; 15: 237-245. doi: 10.1016/j.cocis.2010.03.001. Comprehensive review providing detailed discussion on the application of particle tracking for studying the rheology of interfacial films.

[18**] Tajuelo J, Pastor JM, Rubio MA. A magnetic rod interfacial shear rheometer driven by a mobile magnetic trap. J. Rheol. 2016; 60: 1095-1113. doi: 10.1122/1.4958668. Work introducing a new design of magnetic rod interfacial rheometer allowing for the enhancement of the measurement sensitivity.

[19] Krägel J, Derkatch SR. Interfacial shear rheology. Curr. Opin. Colloid Interface Sci. **2010;** 15: 246-255. doi: 10.1016/j.cocis.2010.02.001.

[20] Erni P, Fischer P, Windhab EJ, Kusnezov V, Stettin H, Lauger J. Stress- and strain-controlled measurements of interfacial shear viscosity and viscoelasticity at liquid/liquid and gas/liquid interfaces. Rev. Sci. Instr. 2003; 74: 4916-4924. doi: 10.1063/1.1614433

[21] Vandebril, S, Franck A, Fuller GG, Moldenaers P, Vermant J. A double wall-ring geometry for interfacial shear rheometry. Rheol. Acta 2010; 49: 131−144. doi: 10.1007/s00397-009-0407-3

[22] Rühs PA, Böni L, Fuller GG , Inglis RF, Fischer O. In-Situ Quantification of the Interfacial Rheological Response of Bacterial Biofilms to Environmental Stimuli. Plos One 2013; 8: e78524. doi: 10.1371/journal.pone.0078524.

[23] Gupta M, Van Hooghten R, Fischer P, ·Gunes DZ, Vermant J. Limiting coalescence by interfacial rheology: over-compressed polyglycerol ester layers. Rheol. Acta 2016; 55: 537-546. doi: 10.1007/s00397-016-0934-7.

[24] Nutting GC, Harkins WD, The Viscosity of Monolayers: a Test of the Canal Viscosimeter. J. Am. Chem. Soc. 1940; 62: 3155-3161. doi: 10.1021/ja01868a073.

[25] Balaraj VS, Zeng PCH, Sanford SP, McBride SA, Raghunandan A, Lopez JM, Hirsa AH. Surface shear viscosity as a macroscopic probe of amyloid fibril formation at a fluid interface. Soft Matter 2017; 13: 1780-1787. doi: 10.1039/c6sm01831a.

[26] Verwijlen T, Moldenaers P, Stone HA, Vermant J. Study of the flow field in the magnetic rod interfacial stress rheometer. Langmuir 2011; 27: 9345−9358. doi: 10.1021/la201109u.

[27**] Brooks CF, Fuller GG, Frank CW, Robertson CR. An Interfacial Stress Rheometer To Study Rheological Transitions in Monolayers at the Air−Water Interface. Langmuir 1999; 15:2450-2459. doi: 2410.1021/la980465r. Work introducing the first a magnetic rod rheometer.

[28] Benmekhbi M, Simon S. Limitations and Applicability of the Interfacial Shear Rheology in the Study of Monolayer Films at the Air-Water Interface. J. Dispers. Sci. Technol. 2014; 35: 150-160. doi: 10.1080/01932691.2012.757197.

[29] Orsi D, Guzmán E, Liggieri L, Ravera F, Ruta B, Chushkin Y, Rimoldi T, Cristofolini L. 2D dynamical arrest transition in a mixed nanoparticle-phospholipid layer studied in real and momentum spaces. Sci. Rep. 2015; 5: 17930. doi:10.1038/srep17930

[30] Orsi D, Rimoldi T, Guzmán E, Liggieri L, Ravera F, Ruta B, Cristofolini L. Hydrophobic Silica Nanoparticles Induce Gel Phases in Phospholipid Monolayers. Langmuir 2016; 32: 4868–4876. doi: 10.1021/acs.langmuir.6b00813.

[31] Goodrich FC. The Theory of Absolute Surface Shear Viscosity. I. Proc. Roy. Soc. 1969; 310: 359-372. doi: 10.1098/rspa.1969.0080.

[32] Goodrich FC. The Hydrodynamical Theory of Surface Shear Viscosity. In Progress in Surface and Membrane Science. Edited by Danielli JF, Rosenberg MD, Cadenhead DA: Elsevier; 1973:151-181. vol 7. doi: 10.1016/B978-0-12-571807-3.50009-0

[33] Reynaert S, Brooks CF, Moldenaers P, Vermant J, Fuller GG. Analysis of the magnetic rod interfacial stress rheometer. J. Rheol. 2008; 52: 261–285. doi: 10.1122/1.2798238.

[34**] Tajuelo J, Rubio MA, Pastor JM. Flow field based data processing for the oscillating conical bob interfacial shear rheometer. J. Rheol. 2018, 62:295-311. doi: 10.1122/1.5012764. First work in which an accurate description of the flow field for a rotational rheometer is used for characterizing the interfacial shear response.

[35] Tajuelo J. Técnicas macro y microscópicas y su aplicación a la caracterización de monocapas de Langmuir. PhD Thesis. Madrid, Spain: Universidad Nacional de Educación a Distancia, 2017.

[36] Zell ZA, Nowbahar A, Mansard V, Leal LG, Deshmukh SS, Mecca JM, Tucker CJ, Squires TM. Surface shear inviscidity of soluble surfactants. Proc. Nat. Acad. Sci. U.S.A. 2014; 111: 3677–3682. doi: 10.1073/pnas.1315991111.

[37] Danov K, Aust R, Durst F, Lange U. Influence of the surface viscosity on the hydrodynamic resistance and surface diffusivity of a large Brownian particle. J. Colloid Interface Sci. 1995; 175: 36-45. doi: 10.1006/jcis.1995.1426.

[38] Danov K, Dimova R, Pouligny B. Viscous drag of a solid sphere stradding a spherical or flat surface. Phys. Fluids 2000; 12: 2711-2722. doi: 10.1063/1.1289692.

[39] Dimova R, Danov K, Pouligny B, Ivanov IB. Drag of a solid particle trapped in a thin film or at an interface: influence of surface viscosity and elasticity. J. Colloid Interface Sci. 2000; 226: 35-43. doi: 10.1006/jcis.2000.6710.

[40] Fischer TM, Dhar P, Heinig P. The viscous drag of spheres and filaments moving in membrane monolayers. J. Fluid Mech. 2006; 558: 451-475. doi: 10.1017/S002211200600022X.

[41] Larsson RG. The Structure and Rheology of Complex Fluids. Oxford, United Kingdom: Oxford University Press, 1999.

[42] Mewis J, Wagner NJ. Thixotropy. Adv. Colloid Interface Sci. 2009, 147: 214-227. doi: 10.1016/j.cis.2008.09.005.

[43*] Maestro A, Bonales LJ, Ritacco H, Fischer TM, Rubio RG, Ortega F. Surface rheology: macro- and microrheology of poly(tert-butyl acrylate) monolayers. Soft Matter 2011, 7:7761-7771. doi: 10.1039/c1sm05225j. Study on the rheological characterization of polymer monolayers in which discrepancies between results obtained using micro- and macro-rheology techniques are evidenced.

[44**] Cicuta P, Donald AM. Microrheology: a review of the method and applications. Soft Matter, 2007; 3: 1449–1455. doi: 10.1039/b706004c. Review devoted of microrheological characterization of sof-matter from fundamental bases to applications.

[45] Koplik J, Maldarelli C. Diffusivity and hydrodynamic drag of nanoparticles at a vapor-liquid interface. Phys. Rev. E 2017; 2: 024303. doi: 10.1103/PhysRevFluids.2.024303

[46] Edwards DA, Brenner H, Wasan DT. Interfacial Transport Processes and Rheology. Boston, United States of America: Butterworth-Heinemann; 1991.

[47] Squires TM, Mason TG. Fluid Mechanics of Microrheology. Annu. Rev. Fluid Mech. 2010; 42: 413-438. doi: 10.1146/annurev-fluid-121108-145608.

[48] Tajuelo J. Unpublished results

[49] Samaniuk JR, Vermant J: Micro and macrorheology at fluid-fluid interfaces. Soft Matter 2014; 10: 7023-7033. doi: 7010.1039/c7024sm00646a.

[50] Elfring GJ, Leal LG, Squires TM. Surface viscosity and Marangoni stresses at surfactant laden interfaces. J. Fluid Mech. 2016; 792: 712-739. doi:10.1017/jfm.2016.96.

[51] Guzmán E, Santini E, Ferrari M, Liggieri L, Ravera F. Effect of the Incorporation of Nanosized Titanium Dioxide on the Interfacial Properties of 1,2-Dipalmitoyl-sn-glycerol-3-phosphocholine Langmuir Monolayers. Langmuir 2017; 33: 10715–10725. doi: 10.1021/acs.langmuir.7b02484.

[52] Guzmán E, Ferrari M, Santini E, Liggieri, L, Ravera F. Effect of silica nanoparticles on the interfacial properties of a canonical lipid mixture. Colloids Surf. B 2015; 136: 971-980. doi: 10.1016/j.colsurfb.2015.11.001.

[53] Hermans E, Vermant J. Interfacial shear rheology of DPPC under physiologically relevant conditions. Soft Matter 2014; 10: 175-186. doi: 10.1039/c3sm52091a.

[54] Guzmán E, Santini E, Zabiegaj D, Ferrari M, Liggieri L, Ravera F. Interaction of Carbon Black Particles and Dipalmitoylphosphatidylcholine at the Water/Air Interface: Thermodynamics and Rheology. J. Phys. Chem. C 2015; 119: 26937–26947.**doi:** 10.1021/acs.jpcc.5b07187.

[55] Guzman E, Santini E, Ferrari M, Liggieri L, Ravera F. Interfacial Properties of Mixed DPPC-Hydrophobic Fumed Silica Nanoparticle Layers. J. Phys. Chem. C 2015; 119:21024-21034. doi: 10.1021/acs.jpcc.5b07258.

[56*] Sosnowski TR. Particles on the lung surface - physicochemical and hydrodynamic effects. Curr. Opin. Colloid Interface Sci. 2018; 36:1-9. doi: 10.1016/j.cocis.2017.12.003. Review on interfacial properties of lipid layers and their correlations to the biological function

[57] Bhamla MS, Chai C, Àlvarez-Valenzuela MA, Tajuelo J, Fuller GG. Interfacial mechanisms for stability of surfactant-laden films. Plos One 2017; 12: e0175753. doi: 10.1371/journal.pone.0175753.

[58*] Kim K, Choi SQ, Zasadzinski JA, Squires TM. Interfacial microrheology of DPPC monolayers at the air–water interface. Soft Matter 2011; 7: 7782-7789. doi: 10.1039/c1sm05383c. Introduction of the magnetic microbutton micro-rheometer on studies of the shear response of monolayers.

[59] Choi SQ, Jang SG, Pascall AJ, Dimitriou MD, Kang T, Hawker CJ, Squires TM. Synthesis of Multifunctional Micrometer-Sized Particles with Magnetic, Amphiphilic, and Anisotropic Properties. Adv. Mater. 2011; 23: 2348–2352. doi: 10.1002/adma.201003604

[60] Zell ZA, Mansard V, Wright J, Kim K, Choi SQ, Squires TM. Linear and nonlinear microrheometry of small samples and interfaces using microfabricated probes. J. Rheol. 2016; 60:141. doi: 10.1122/1.4937931

[61] Guzmán E, Orsi D, Cristofolini L, Liggieri L, Ravera F. 2D DPPC Based Emulsion–like Structures Stabilized by Silica Nanoparticles. Langmuir 2014; 30: 11504–11512. doi: 10.1021/la502183t.

[62] Hui S, Yu H, Xu Z, Bittman R: Microdomains in Polymerizable Diacetylenic Phosphatidylcholine Monolayers. In Synthetic Microstructures in Biological Research. Schnurr JM, Peckerar MS (ed.). New York, United States of America: Springer US, 1992:17-27. doi: 10.1007/978-1-4899-1630-3_2

[63] Espinosa G., López-Montero I, Monroy F, Langevin D. Shear rheology of lipid monolayers and insights on membrane fluidity. Proc. Nat. Acad. Sci. U.S.A. 2011: 108; 6008–6013. doi: 10.1073/pnas.1018572108.

[64] Choi SQ, Steltenkamp S, Zasadzinski JA, Squires TM. Active microrheology and simultaneous visualization of sheared phospholipid monolayers. Nat. Commun. 2011; 2: 312. doi: 10.1038/ncomms1321.

[65] Shlomovitz R, Evans AA, Boatwright T, Dennin M, Levine AJ. Measurement of Monolayer Viscosity Using Noncontact Microrheology. Phys. Rev. Lett. 2013; 110: 137802. doi: 10.1103/PhysRevLett.110.137802.

[66] Shlomovitz R, Evans AA, Boatwright T, Dennin M, Levine AJ. Probing interfacial dynamics and mechanics using submerged particle microrheology. I. Theory. Phys. Fluids 2014; 26: 071903. doi: 10.1063/1.4886996.

[67] Boatwright T, Dennin M, Shlomovitz R, Evans AA, Levine AJ. Probing interfacial dynamics and mechanics using submerged particle microrheology. II. Experiment. Phys. Fluids 2014; 26: 071904. doi: 10.1063/1.4887084

[68] Park CY Ou-Yang HD, Kim MW. Interface shear microrheometer with an optically driven oscillating probe particle. Rev. Sci. Instrum. 2011; 82: 094702. doi: 10.1063/1.3627410,

[69] Kim K, Choi SQ, Zell ZA, Squires TM, Zasadzinski JA. Effect of cholesterol nanodomains on monolayer morphology and dynamics. Proc. Nat. Acad. Sci. U.S.A. 2013; 110: E3054–E3060. doi: 10.1073/pnas.1303304110.

[70] Choi SQ, Kim K, Fellows CM, Cao KD, Lin B, Lee KYC, Squires TM, Zasadzinski JA. Influence of Molecular Coherence on Surface Viscosity. Langmuir 2014; 30: 8829–8838. doi: 10.1021/la501615g.

[71] Guzman E, Liggieri L, Santini E, Ferrari M, Ravera F. Mixed DPPC-cholesterol Langmuir monolayers in presence of hydrophilic silica nanoparticles. Colloids Surf. B 2013; 105:284-293. doi: 10.1016/j.colsurfb.2013.01.020.

[72] Sachan AK, Choi SQ, Kim KH, Tang Q, Hwang L, Lee KYC, Squires TM, Zasadzinski JA. Interfacial rheology of coexisting solid and fluid monolayers. Soft Matter 2017; 13: 1481-1492. doi: 10.1039/c6sm02797k.

[73] Ding JQ, Warriner HE, Zasadzinski JA. Viscosity of two-dimensional suspensions. Phys. Rev. Lett. 2002; 88: 168102. doi: 10.1103/PhysRevLett.88.168102.

[74] Ghazvini S, Ricke B, Zasadzinski JA, Dhar P. Monitoring phases and phase transitions in phosphatidylethanolamine monolayers using active interfacial microrheology. Soft Matter 2015; 11:3313-3321. doi: 10.1039/c4sm02900c.

[75] Zell ZA, Nowbahar A, Mansard V, Leal LG, Deshmukh SS, Mecca JM, Tucker CJ, Squires TM. Surface shear inviscidity of soluble surfactants. Proc. Nat. Acad. Sci. U.S.A. 2014; 111: 3677–3682. doi: 10.1073/pnas.1315991111.

[76] Martínez-Pedrero F, Tajuelo J, Sánchez-Puga P, Chulia-Jordan R, Ortega F, Rubio MA, Rubio RG. Linear shear rheology of aging b-casein films adsorbing at the air/water interface. J. Colloid Interface Sci. 2018; 511: 12-20. doi: 10.1016/j.jcis.2017.09.092

[77] Risovi D, Frka S, Kozarac Z. Application of Brewster angle microscopy and fractal analysis in investigations of compressibility of Langmuir monolayers. J. Chem. Phys. 2011; 134: 024701. doi: 10.1063/1.3522646.

[78] Benmekhbi M, Simon S. Limitations and Applicability of the Interfacial Shear Rheology in the Study of Monolayer Films at the Air-Water Interface. J. Dispersion Sci. Tech. 2014; 35:150–160. doi: 10.1080/01932691.2012.757197.

[79] Wu XZ, Sirota EB, Sinha SK, Ocko BM, Deutsch M. Surface Crystallization of Liquid Normal-Alkanes. Phys. Rev. Lett. 1993: 70; 958-961. doi: 10.1103/PhysRevLett.70.958.

[80] Tajuelo J, Guzmán E, Ortega F, Rubio RG, Rubio MA. Phase Diagram of Fatty Acid Langmuir Monolayers from Rheological Measurements. Langmuir 2017; 33: 4280-4290. doi: 10.1021/acs.langmuir.7b00613. ¡
[81] Kaganer VM, Möhwald H, Dutta, P. Structure and phase transitions in Langmuir monolayers. Rev. Mod. Phys. 1999; 71: 779-819. doi: 10.1103/RevModPhys.71.779.

[82] Ghaskadvi RS, Ketterson JB, Dutta P. Nonlinear Shear Response and Anomalous Pressure-Dependence of Viscosity in a Langmuir Monolayer. Langmuir 1997; 13: 5137−5140. doi: 10.1021/la970036d.

[83] Copeland LE, Harkins WD, Boyd GE. A Superliquid in Two Dimensions and a First Order Change in a Condensed Monolayer II. Abnormal Viscosity Relations of Alcohol Monolayers in Condensed Liquid Phases. J. Chem. Phys. 1942; 10: 357. doi: 10.1063/1.1723735.

[84] Maestro A, Jones DW, de Rojas-Sanchez CS, Guzmán E, Duits Michael HG, Cicuta P. Tuning interfacial properties and processes by controlling the rheology and structure of PNIPAM particles at air/water interfaces. Langmuir 2018; 34:. doi: 10.1021/acs.langmuir.7b03879.